First-principles study of electron-phonon coupling in hole- and electron-doped diamonds in the virtual crystal approximation

Yanming Ma,[1,3] John S. Tse,[2,3] Tian Cui,[1] Dennis D. Klug,[3] Lijun Zhang,[1] Yu Xie,[1] Yingli Niu,[1] and Guangtian Zou[1]
[1]*National Laboratory of Superhard Materials, Jilin University, Changchun 130012, People's Republic of China*
[2]*Department of Physics and Engineering Physics, University of Saskatchewan, Saskatoon, Canada, S7N 5A2*
[3]*Steacie Institute for Molecular Sciences, National Research Council of Canada, Ottawa, Ontario, Canada, K1A 0R6*
(Received 31 January 2005; revised manuscript received 19 May 2005; published 22 July 2005)

The electronic structure, lattice dynamics, and the electron-phonon coupling (EPC) in hole (p)-doped and electron (n)-doped diamonds have been extensively investigated using *ab initio* methods with the virtual crystal approximation. The calculations of p-doped diamond correctly reproduced all the essential properties of B-doped diamond such as the increase of lattice constant and the redshift of the Raman spectrum with increasing dopant concentration, and the pressure-induced decrease of T_c. The analysis of the spectral function for p-type diamond has shown that optical phonon modes dominate the EPC. From the theoretical prediction of n-doped diamond, it is indicated that the metallic n-doped diamond might be a good superconductor. It is found that the λ in n-doped diamond increases with the dopant concentration, resulting from the softening of optical phonon modes and the increase of density of states at Fermi level. At a doping level $>2\%$, the λ in n-doped diamond is higher than that in p-doped diamond. Phonon linewidth and frozen phonon calculations in n-doped diamond suggested that the longitudinal optical phonon mode contributes mainly to the EPC. The possible mechanism of the predicted superconductivity in n-doped diamond has been discussed.

DOI: 10.1103/PhysRevB.72.014306 PACS number(s): 63.20.Kr

I. INTRODUCTION

Pure and doped diamonds have attracted much technological attention because of their high carrier mobility, high thermal conductivity, high breakdown field, low dielectric constant, and wide band gap. The creation of such devices requires the fabrication of low-resistivity n-type and p-type materials by doping diamond with donor and acceptor impurities, respectively. As a representative acceptor in p-type diamond, small B atoms can be incorporated substitutionally into diamond with high reproducibility and high enough concentration to be useful for electronic devices. B dopes holes into a shallow acceptor level close to the top of the valence band. Electrical transport studies show that at low B concentrations ($10^{17}-10^{19}$ cm^{-3}) doped diamond is semiconducting with an activation energy of $\sim$0.35 eV. Increasing the B concentration to 10^{20} cm^{-3} gradually decreases the activation energy, and for B concentrations $\geqslant 10^{20} \sim 10^{21}$ cm^{-3}, the electrical conductivity becomes metallic. Recently, B-doped diamond was found to be a superconductor with a critical temperature (T_c) of 2.3 K.[1] Additional confirmation has been provided recently by Takano *et al.*,[2] Sidorov *et al.*,[3] and Bustarret *et al.*[4] This observation is a breakthrough finding, not only due to the obvious practical implications, but also to the scientific importance. The mechanism of the superconductivity in B-doped diamond has been explored extensively by several theory groups.[5–9] Boeri *et al.*[5] and Lee *et al.*[6] used the virtual crystal approximation (VCA) to probe the nature of this superconductivity. It was suggested that the holes in the valence band couple strongly with the optical phonons, analogous to what has found in MgB_2. Xiang *et al.*[7] and Blase *et al.*[8] used the supercell method and discussed the effect of boron impurity on the superconductivity by including explicitly B as an impurity. Based on a resonating valence band model, Baskaran[9] demonstrated the importance of electron correlation to the superconductivity in an impurity band. It is important to mention that both the supercell and VCA model yield essentially the same conclusion that the main mechanism responsible for the superconductivity is attributed to a very localized electron-phonon coupling (EPC) of a zone center optic phonon mode, which is softened as a result of B-doping.

Much experimental[10–14] and theoretical[15] effort has been paid to search for n-type diamonds for potential electronic applications. Experimentally, n-type diamonds with In, Cd, Hf,[10] P,[11,12] N,[13] Li, and Na (Ref. 14) as the donors have been successfully synthesized. It should be noted that at low doping levels and to a first approximation, the donors donate electrons to the conduction band of the diamond framework. It is known that if the dopant concentration (dc) reaches a critical value, then the doped diamond will exhibit metallic behavior.[16] In view of the recent characterization of superconductivity in p-doped diamond,[1] thus, it is relevant (i) do the excess electrons in the conduction band couple strongly with the phonons and result in a superconducting state in metallic n-type diamond? If so, (ii) is the mechanism of EPC in n-type diamond similar to that in p-type diamond?

In order to gain a comprehensive look into the entire superconducting behavior of p-doped and n-doped diamonds, and in view of the very low metallic dc [e.g., $(2-4.9)\times 10^{21}$ cm^{-3} in B-doped diamond] and that superconductivity is generally considered as a bulk property, we employed the VCA to model the electronic state, vibrational properties, and the EPC for both metallic p-type and metallic n-type diamonds with a small amount of acceptors and donors, respectively. The first focus of this study is to expand previous p-doped studies to include a detailed investigation on the effects of doping concentration and pressure on the super-

TABLE I. Calculated lattice constants (a_0), bulk modulus (B_0), average phonon frequency ($\langle\omega\rangle$), density of states at Fermi level [$N(0)$], electron-phonon coupling coefficient (λ), logarithmically averaged characteristic phonon frequency ($\omega_{\log}$), and superconducting transition temperature (T_c) for *p*-doped diamonds with e_v=3.99, 3.98, 3.96, and 3.94, respectively, and for *n*-doped diamonds with e_v=4.01, 4.02, 4.03, 4.04, and 4.05, respectively. The experimental data in parentheses for lattice constant (Ref. 1) and bulk modulus (Ref. 22) in pure diamond are also listed for the comparison with the theoretical results. The estimated dopant concentration (*dc*) in two units (% and 10^{21} cm^{-3}) is also listed for the different electron configuration e_v.

Diamond	e_v	*dc* (%)	*dc* ($\times 10^{21}$ cm^{-3})	a_0 (a.u.)	B_0 (GPa)	$\langle\omega\rangle$ (THz)	$N(0)$ (states/spin/Ry/unit)	λ	$\omega_{\log}$ (K)	T_c(K) $\mu^*=0.066$	T_c(K) $\mu^*=0.1$
Pure	4.00			6.6863 (6.7395[a])	441.0 (443[b])	29.59					
n-type	4.01	1.0	1.81	6.6843	443.3	29.22	0.67	0.15	1456	0.0	0.0
	4.02	2.0	3.62	6.6836	443.8	28.81	0.97	0.25	1389	0.7	0.1
	4.03	3.0	5.43	6.6830	444.2	28.39	1.18	0.33	1349	4.5	1.5
	4.04	4.0	7.24	6.6824	444.6	27.92	1.37	0.41	1319	12.4	6.4
	4.05	5.0	9.05	6.6819	444.8	27.47	1.55	0.49	1291	23.2	14.5
p-type	3.99	1.0	1.80	6.6896	439	29.44	0.54	0.18	1623	0.01	0.0
	3.98	2.0	3.60	6.6948	436	29.10	0.73	0.25	1570	0.74	0.1
	3.96	4.0	7.16	6.7060	431	28.47	0.99	0.34	1502	7.91	2.2
	3.94	6.0	10.5	6.71739	426	27.82	1.19	0.40	1446	12.3	6.1

[a]The experimental data is taken from Ref. 1.
[b]The experimental data is taken from Ref. 22.

conducting critical temperature. The current study correctly reproduced the pressure dependence on T_c and confirmed that an increase in doping concentration results in the increase of T_c. The second subject of this investigation is to address the above described two questions for *n*-doped diamond. It is predicted that the heavily *n*-doped diamond might also be a good superconductor and the large EPC in *n*-doped diamond is mainly from the longitudinal optical phonon mode.

II. COMPUTATIONAL DETAILS

Pseudopotential plane-wave *ab initio* calculations were performed within the framework of density functional theory.[17] The generalized gradient approximation exchange-correlation functional was employed.[18] A Troullier-Martins[19] norm-conserving scheme is used to generate the "virtual crystal" pseudopotential for C at different electron concentrations. To maintain charge neutrality, the nuclear charge of the pseudo-atom was also reduced (or increased) by the same amount as for the depleted (or excess) valence electrons, thus instead of a normal C valence electron count of 4, virtual C atoms were created with fractional electrons according to different doping concentrations. For *p*-doped diamond, four concentrations with effective numbers of valence electrons (e_v) of 3.99*e*, 3.98*e*, 3.96*e*, and 3.94*e*, corresponding to 0.01, 0.02, 0.04, and 0.06 doped holes per C atom are studied. For *n*-doped diamond, five concentrations with e_v of 4.01*e*, 4.02*e*, 4.03*e*, 4.04*e*, and 4.05*e* were studied, corresponding to 0.01, 0.02, 0.03, 0.04, and 0.05 doped electrons per C atom. Both for *p*-doped and *n*-doped diamonds, convergence tests gave a kinetic energy cutoff, E_{cutoff} of 55 Ry and a $16\times16\times16$ Monkhorst-Pack (MP) grid for the electronic Brillouin Zone (BZ) integration. Theoretical equilibrium lattice constants are determined by fitting the total energies as a function of volume to the Murnaghan equation of state.[20]

The lattice dynamics of pure, *p*-type, and *n*-type diamonds were calculated using the linear-response method.[17] A $16\times16\times16$ MP *k* mesh was found to yield phonon frequencies converged to within 0.05 THz, and this was used in all calculations. A $4\times4\times4$ *k* mesh in the first BZ was used in the interpolation of the force constants for the phonon dispersion curve calculations. The technique in the calculation of EPC for *n*-type and *p*-type diamonds has been described in detail in our previous publication.[21] A MP $32\times32\times32$ *k* mesh is chosen to ensure *k*-point sampling convergence with Gaussians of width 0.03 Ry, which approximates the zero width limits in the calculations of phonon linewidth and EPC parameter λ.

III. RESULTS AND DISCUSSIONS

Assuming the replacement of a C atom with an acceptor atom (e.g., boron doping) or a donor atom (e.g., nitrogen and phosphorus doping) contributes exactly one hole or one electron in the valance or conduction band, the estimated *dc* is summarized in Table I. It is noteworthy that these *dc*'s are within the same magnitude of the metallic B-doped diamond [$(2-4.9)\times10^{21}$ cm^{-3}].[1] The calculated lattice constants and bulk moduli with *dc* for pure, *p*-type, and *n*-type diamonds are also listed in Table I. It is clear that the calculations for *p*-doped diamond correctly predict an increase of lattice con-

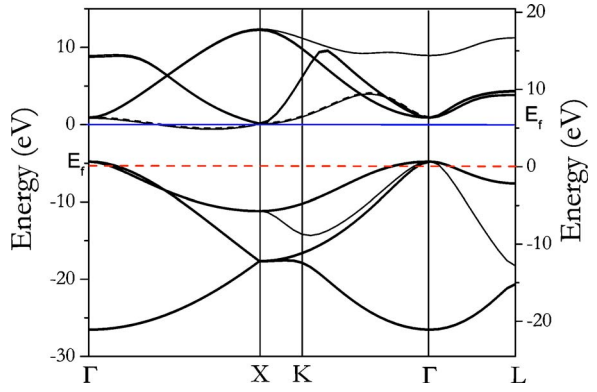

FIG. 1. (Color online) The calculated band structures for p-doped diamond with $e_v=3.98$ (right label) and n-doped diamond with $e_v=4.02$ (left label). The blue solid line located in the conduction band denotes the Fermi level for n-doped diamond, while the red dashed line located in the valence band denotes the Fermi level for p-doped diamond.

stant with increasing dc, in agreement with the theoretical predictions[5,7] and the experimental observations.[1,23,24] The band structure of p-doped diamond for $e_v=3.98$ is shown in Fig. 1. One observes that the Fermi level is located in the valence band around the Γ point of the BZ, resulting from the introduction of holes. Since the valence bands are not fully occupied, p-doped diamonds are weak metals. Note also that the introduction of holes reduces the valence electron density at the zone center and weakens the chemical bonding as evidenced by the decrease of the bulk modulus with dc as shown in Table I. The electron density of states (DOS) for p-doped diamond at the Fermi level, $N(0)$, increases with dc as presented in Table I. For n-doped diamond, we find that the calculated unit cell size decreases slightly with increasing dc, indicating a bonding contraction in a C sp^3 network. There is also a noticeable increase in the bulk modulus with increasing dc. This behavior is opposite from that observed in p-type diamond. It should be pointed out that the theoretically proposed β-C_3N_4 and cubic C_3N_4 within C in a four-neighbor sp^3 framework as in the diamond phase have larger bulk moduli than that of diamond.[25] At ambient condition, the C—N bond lengths are 1.456 and 1.460 Å for beta-C_3N_4 and cubic C_3N_4,[25] respectively, shorter than the C—C bond length of 1.544 Å in diamond. This fact supports the current n-doped calculation. The electron band structure for n-doped diamond with $e_v=4.02$ as shown in Fig. 1 reveals that the electrons introduced into the conduction band help to increase the electron density near the X point at the Fermi level and making n-doped diamond weakly metallic. The electron DOS for n-doped diamond at the Fermi level, $N(0)$, increases with dc as shown in Table I, similar to that of p-doped diamond. It should be pointed out that the apparent difference in the electronic behaviors of the two doped systems as indicated in Fig. 1 may result in a significant difference in the physical properties of lattice dynamics and the EPC.

The theoretical phonon dispersion curve and the experimental phonon data[26] for pure diamond are shown in Fig. 2. The calculated phonon dispersion curve is in excellent agreement with the experimental measurements, lending strong support for the validity of this calculation. The phonon dispersion curves for pure diamond and p-doped diamonds with $e_v=3.98$ and 3.96 are shown in Fig. 3(a). For comparison, the phonon density of states (DOS) for these three systems is also shown. The change of phonon dispersion with dc is

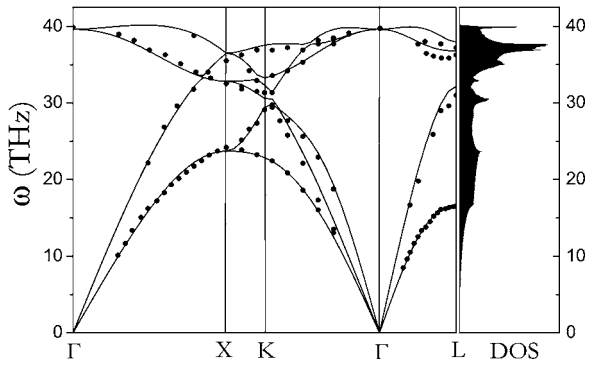

FIG. 2. The comparison of the calculated phonon dispersion curves (solid line) with the experimental data (symbols) from Ref. 26 for pure diamond is shown in left figure. The theoretical phonon density of states is shown in the right figure.

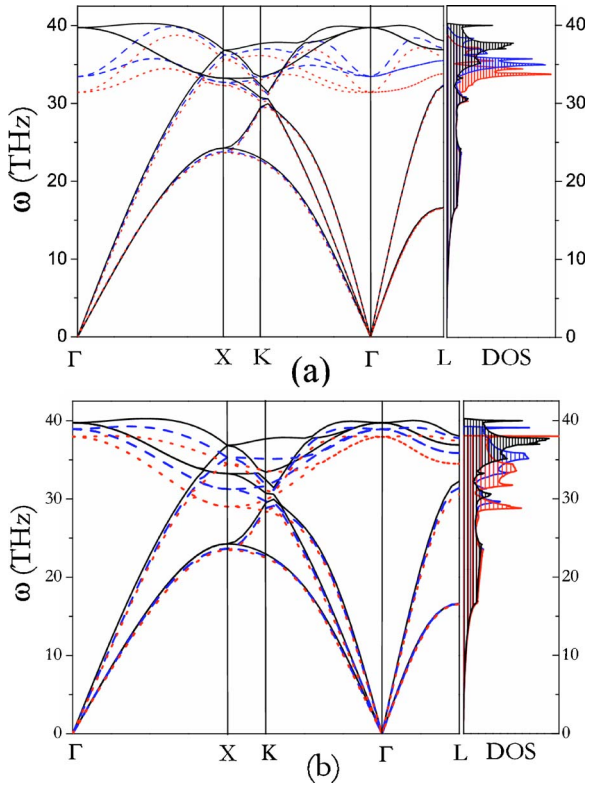

FIG. 3. (Color online) (a) The comparison of the calculated phonon dispersion curves in pure (black solid line) and p-doped diamonds with $dc=2\%$ (blue dashed line) and 4% (red dotted line) in the left figure, together with the corresponding phonon density of states in the right figure. (b) The comparison of the calculated phonon dispersion curves in pure (black solid line) and n-doped diamonds with $dc=2\%$ (blue dashed line) and 4% (red dotted line) in the left figure, together with the corresponding phonon density of states in the right figure.

significant near the zone center. This observation is in agreement with the predictions of the previous VCA model[5] and the supercell model.[7,8] The acoustic phonon modes do not show a clear dependence on *dc*. In contrast, the frequency of the optical phonons decreases significantly with increased doping. The theoretical results are consistent with the redshift of the optic band observed in B-doped diamonds from Raman measurements.[1] At a *dc* of $e_v=3.99$, the calculated shift of the zone center optical mode[27] with respect to pure diamond of $\sim 80\ \mathrm{cm}^{-1}$ is to be compared with the observed shift of $\sim 32\ \mathrm{cm}^{-1}$.[1] Since we account for every extra hole to be mobile, the theoretical holes mobility is the upper limit of the experimental one. Therefore the overestimated frequency shift is as not unexpected. Note also that the theoretical model assumes a homogenous distribution of B in doped diamond. In actual experiments B may not be doped evenly into diamond. For a clear view of the averaged phonon dependence on *dc*, the decrease of average phonon frequencies $\langle\omega\rangle$ for *p*-doped diamonds with *dc* is listed in Table I.

The phonon dispersion curves for *n*-doped diamonds with $e_v=4.02$ and 4.04 are compared with pure diamond in Fig. 3(b). For comparison, the phonon DOS for these three systems is also shown. As indicated in Fig. 3(b), the phonon dispersion curves of *n*-type diamond show a softening behavior with an increase in *dc*. The most noticeable softening in phonon frequency is found at the *X* point in the BZ. This observation is totally different from previously found for *p*-type diamond where the largest phonon softening only occurs at the zone center. The lattice vibration at the zone center can be determined from the Raman spectrum. Koizumi *et al.*[12] have measured the Raman spectra for pure and *n*-doped (with phosphorus) diamond thin films. A small redshift relative to the pure diamond thin film was observed in the doped samples. This observation provides support for the validity of the present theoretical approaches. Unfortunately, due to the very low *dc* (~ 1000 ppm) used in the Raman experiments[12] for *n*-doped diamond, it is not possible to make a quantitative comparison between theory and experiment. The dramatic changes of phonon DOS for high frequency modes with doping [Fig. 3(b)] indicate that the *n*-doping has a significant effect on the lattice dynamics. The calculated average phonon frequencies $\langle\omega\rangle$ for *n*-doped diamonds are presented in Table I. The decrease in $\langle\omega\rangle$ with *dc* is the consequence of the phonon softening behavior discussed above.

The calculated EPC parameter λ's for *p*-doped diamonds with *dc*, together with the previous VCA results by Boeri *et al.*,[5] are shown in Fig. 4. It is clearly seen that the current calculation is in excellent agreement with the previous VCA calculation.[5] It is predicted that λ will increase significantly with increasing *dc*, thus resulting in an increase of the superconducting transition temperature, in agreement with the suggestions by Boeri *et al.*[5] and Xiang *et al.*[7] At the experimental B-doping concentration of $4.9\times 10^{21}\ \mathrm{cm}^{-3}$, $e_v=3.972$, a predicted $\lambda=0.29$ is obtained by the interpolation of the calculated data point in Fig. 4. This value is reasonably close to the 0.2 (Ref. 1) derived experimentally from the measured T_c using a simplified form of the McMillan equation,[28] which neglected the Coulomb pseudopotential

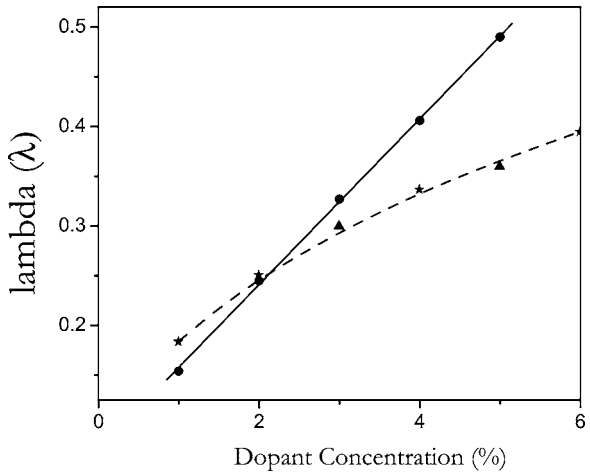

FIG. 4. The variation of electron-phonon coupling parameter λ with dopant concentration. Solid stars are the current VCA results for *p* doped diamonds and solid up triangles are the previous VCA results for *p* doped diamonds taken from Ref. 5. Solid circles are the current VCA results for *n*-doped diamond. The solid line through the data is a linear fit. The dashed line is a B-spline fit to the data.

μ^*. In this study, a more rigorous form $T_c=\omega_{\log}/1.2\exp[-1.04(1+\lambda)/\lambda-\mu^*(1+0.62\lambda)]$ (Ref. 29) was used to estimate the T_c. Instead of the conventional choice of 0.1, a smaller value of 0.066 for μ^* is obtained by equating the experimentally measured T_c (2.3 K) with those of theoretical λ (0.29) and characteristic frequency $\omega_{\log}$ (~ 1543 K). The characteristic frequency listed in Table I at each e_v was obtained from the respective spectral function.[29] Using this μ^* and theoretical λ and $\omega_{\log}$, the T_c at different *dc* considered here is presented in Table I.

The calculated EPC λ's for *n*-type diamonds at different *dc* are also shown in Fig. 4 and listed in Table I. The calculations also predicted that λ should increase significantly with increasing *dc*. Assuming other factors remain unchanged, the observation implies that the superconducting transition temperature ought to increase with *dc*, similar to the trend predicted for *p*-type diamond. The λ in *n*-doped diamond shows an almost linear relationship with increasing *dc*. A linear fit to the calculated λ with *dc* in *n*-doped diamond yields $\lambda=(0.075\pm 0.004)+(0.083\pm 0.001)\times dc$. Therefore λ increases with *dc* at a rate of $0.083/dc$. As indicated in Fig. 4, when the *dc* is below 2%, λ in *p*-doped diamond is larger than that of *n*-doped diamond. While when the *dc* is higher than 2%, λ in *n*-doped diamond is higher than that of the corresponding *p*-doped diamond. At the highest concentration studied here $dc=5\%$ the λ of *n*-type diamond is larger than that in *p*-doped diamond by 0.19 as shown in Fig. 4. Assuming the validity of applying the equated μ^* of ~ 0.066 in *p*-type diamond to the system of *n*-doped diamond, we can estimate the T_c's at different *dc* (Table I) for *n*-type diamond employing the characteristic frequency $\omega_{\log}$ evaluated from the spectral function as listed in Table I. It is significant to note that in *n*-doped diamond, the predicted T_c at $dc=5\%$ is 23.2 K, which is significantly higher than the estimated value of ~ 12 K at $dc=6\%$ in *p*-doped diamond. Note that

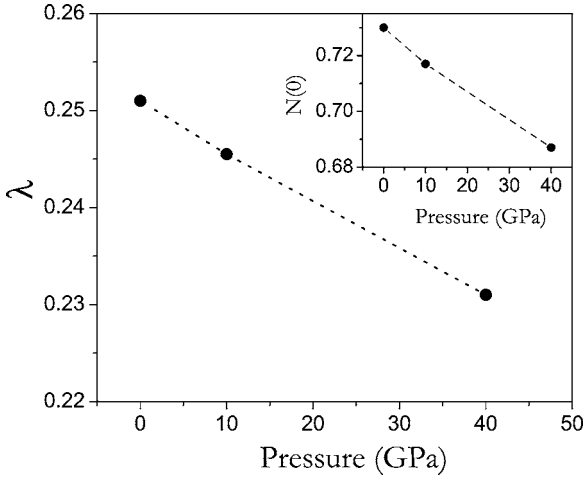

FIG. 5. The pressure dependence of λ for p-doped diamond with $e_v=3.98$. The inset shows the variation of $N(0)$ (in the unit of states/spin/Ry/unit) with pressure. The dotted lines through the theoretical data points are a guide for the eye.

for a comparison, T_c's are also calculated for p-doped and n-doped diamonds using an empirical value of $\mu^*=0.1$ as listed in Table I.

The increased trend of λ with dc for p-doped and n-doped diamonds can be understood as follows. The EPC λ can be approximated by $\lambda \approx N(0)\langle I^2\rangle/(M\langle\omega^2\rangle)$,[29] where $\langle I^2\rangle$ is the average square of the electron-phonon matrix element, which is related to the phonon linewidth, M is the ionic mass, and $\langle\omega^2\rangle$ is a characteristic phonon frequency averaged over the phonon spectrum. The addition of a small amount of donor atoms or acceptor atoms to diamond has two significant effects. First, it affects the phonon spectrum essentially by decreasing the phonon modes (*vide infra*). Second, the p-doped and n-doped diamonds become more metallic with increasing dc as indicated by the increase in $N(0)$ (see Table I). Since the calculated phonon linewidth does not change appreciably with dc, the increase of λ with dc for the doped diamond is attributed to the combined effect of phonon softening and the increased electron density of states at the Fermi level.

The effect of pressure on λ for p-doped diamond with $e_v=3.98$ ($dc=2\%$) is depicted in Fig. 5. The λ of p-doped diamond was found to decrease with pressure, in agreement with the experimental observation in B-doped diamond.[1] At ambient pressure, the T_c is estimated to be 0.74 K for $e_v=3.98$. At 10 GPa, the calculated λ of 0.246 corresponds to a T_c of 0.62 K and at 40 GPa the calculated λ of 0.23 results in a T_c of 0.33 K. The theory predicted an almost negative linear dependence of T_c with pressure with a coefficient of −0.012 K/GPa. This value is reasonably compared with the experimental measurement of −0.062 K/GPa (Ref. 1) at $e_v=3.972$. The smaller calculated pressure coefficient is understandable since this quantity is strongly dependent on the dc. The T_c of 2.3 K at the experimental concentration $e_v=3.972$ is reduced to 0.74 K at $e_v=3.98$. Therefore the pressure gradient is expected to increase at the experimental concentration. It is noteworthy that the McMillan equation is an empirical formula and can only provide qualitative results.

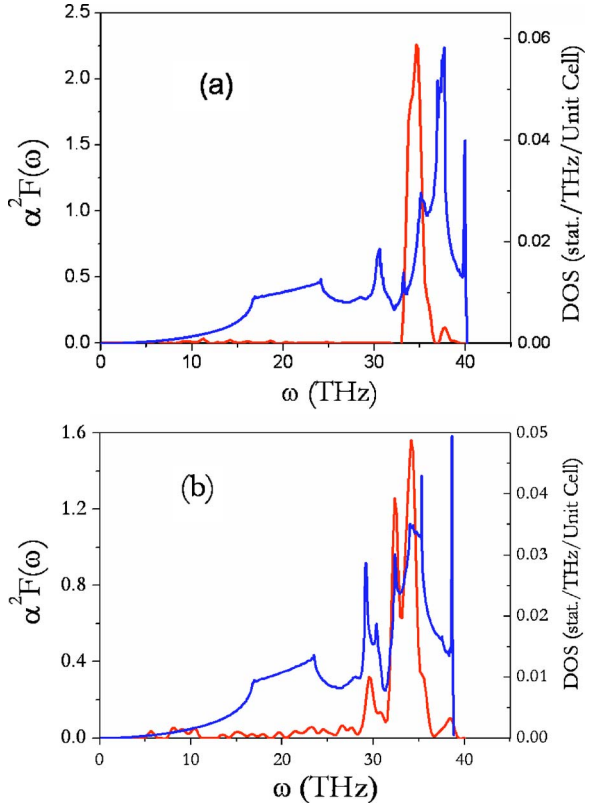

FIG. 6. (Color online) (a) The electron-phonon coupling spectral function $\alpha^2F(\omega)$ (red solid line) with the left label and phonon density of states (blue dashed line) with the right label for p-doped diamond with $e_v=3.98$. (b) The electron-phonon coupling spectral function $\alpha^2F(\omega)$ (red solid line) with the left label and phonon density of states (blue dashed line) with the right label for n-doped diamond with $e_v=4.03$.

Significantly, the present calculations correctly indicate that T_c should have a strong linear dependence on pressure. As shown in the inset of Fig. 5, $N(0)$ decreases with increasing pressure. This behavior combined with an increase in phonon frequency at high pressure contributes to the decrease in T_c.

The spectral functions $\alpha^2F(\omega)$ evaluated as a weighted sum over linewidths of individual phonons for p-doped diamond with $e_v=3.98$ [Fig. 6(a)] and n-doped diamond with $e_v=4.03$ [Fig. 6(b)] are compared to the corresponding phonon DOS in Fig. 6. Usually, the phonon DOS and $\alpha^2F(\omega)$ profiles are quite similar in many materials; they are strikingly different in p-type and n-type diamonds. From the spectral function for these two cases, one observes that the low frequency phonons almost do not contribute to the EPC. In contrast, the optical phonon modes for p-doped diamond in the region of 33.0–36.7 THz contribute significantly to the EPC as shown in Fig. 6(a), in agreement with the observation by Boeri *et al.*[5] and Xiang *et al.*[7] While for n-doped diamond high frequency modes in the region of 28.5–36.3 THz contribute mostly to EPC as indicated in Fig. 6(b).

The phonon linewidth which characterizes the EPC along several high symmetry directions for p-doped diamond with $e_v=3.98$ is presented in Fig. 7(a). The calculated phonon linewidths of the acoustic modes are very small at all $\boldsymbol{q}$ vec-

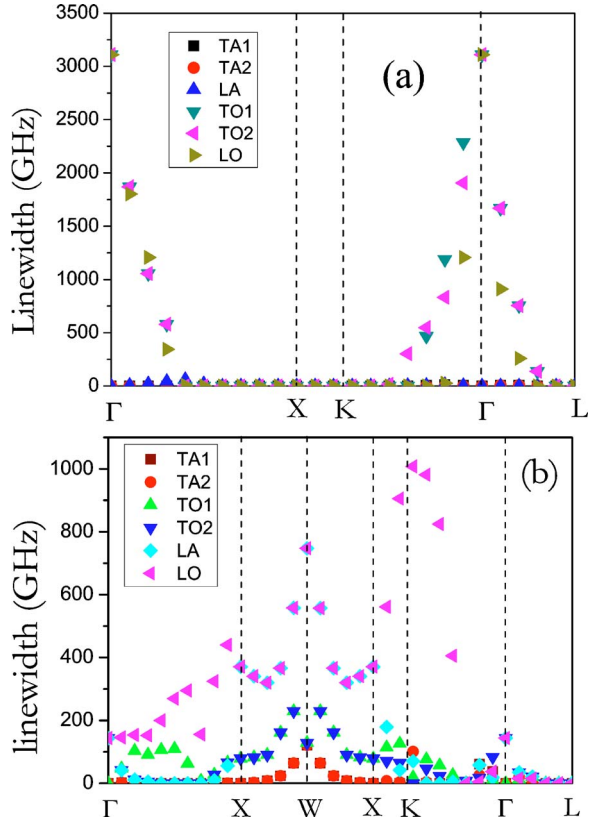

FIG. 7. (Color online) (a) The phonon linewidth due to electron-phonon coupling for *p*-doped diamond at e_v=3.98 along several high symmetry directions in the BZ. The data points (solid left and down triangles) are the transverse optical phonon modes, while solid right triangles represent the longitudinal optical phonon modes. (b) The phonon linewidth due to electron-phonon coupling of *n*-doped diamond with e_v=4.03 along several high symmetry directions in the BZ. The calculated data points presented in the magenta solid left triangles and cyan solid diamond are for longitudinal optical and acoustic phonon modes, respectively. The data points (solid up and down triangles) are the transverse optical phonon modes, while solid squares and circles represent the transverse acoustic phonon modes.

tors, indicating negligible contributions to EPC from these modes. This is consistent with the interpretation of the spectral function $\alpha^2F(\omega)$ shown in Fig. 6(a). The phonon linewidths for the optical modes are comparatively large and decrease rapidly away from the zone center. Less than half way to the zone boundary, the phonon linewidths approach zero indicating that the dominant EPC is localized at the BZ center.[5,6] It is noteworthy that in the current VCA calculated spectral function [Fig. 6(a)] for *p*-doped diamond with e_v =3.98, a strong band at 34 THz (1132 cm^{-1}) and a weaker band at 38 THz (1265 cm^{-1}) were predicted. These features are in agreement with the supercell calculated spectral function[8] where a strong band at 1025 cm^{-1} and a weaker band at 1220 cm^{-1} were observed.

The calculated phonon linewidth for *n*-doped diamond with e_v=4.03 is presented in Fig. 7(b). It is found that the phonon linewidth for the transverse acoustic (TA) phonon mode is very small at all $\boldsymbol{q}$ vectors, indicating a negligible

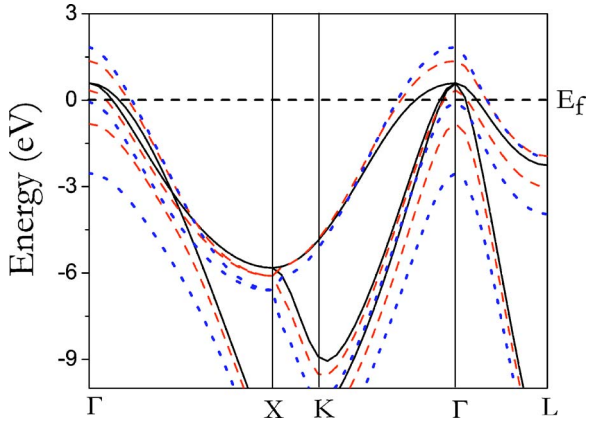

FIG. 8. (Color online) Calculated band structure for *p*-doped diamond at e_v=3.98 with displacement along one of the triply degenerate optical vibration modes. The magnitude of the atomic displacement is μ=0.0354 Å (red dashed lines) and 0.0708 Å (blue dotted lines), respectively.

contribution to EPC. In contrast, transverse optical (TO) phonon modes have a noticeable contribution to EPC along the Γ-*X*-*W*-*X* directions and the longitudinal acoustic (LA) phonon modes only contribute in the *X*-*W* direction. Note that at *X* point the TA and LO phonon modes are degenerated. The very large phonon linewidth shown in Fig. 7(b) is mainly derived from high frequency LO phonon modes. These results are also reflected in the profile of the spectral function. Therefore the LO phonon modes dominate the EPC in *n*-doped diamond.

Electronic response to a lattice vibration characterizes the strength of EPC for a given phonon vibration mode.[30] For undoped diamond, the highest occupied electronic band at the zone center has triply degenerate T_{1u} symmetry. The removal of electrons from this band through *p*-doping creates an orbitally degenerate state and would be subjected to large electronic coupling with the lattice vibrations. For *p*-doped diamond, the dominant EPC is localized at the BZ center. Thus a supercell frozen phonon calculation is performed for an optical phonon at the zone center Γ point to probe the electronic changes with a certain atomic displacement. The variations of the calculated electronic band structure with several small displacements are shown in Fig. 8. It is found that the vibration effect is strongest at the Γ point where the triple degeneracy of the band is broken and opens a "gap" of almost 3 eV, characterizing the origin of the superconductivity in B-doped diamond. The change in the band structure is evidently much weaker at other symmetry points. This observation is in good accord with phonon linewidth calculations, which show that the main contribution to the EPC is the vibration near the Γ point. The current frozen phonon calculation for *p*-doped diamond agrees well with the previous VCA results.[5,6]

For *n*-doped diamond, since the LO phonon mode was found to have a significant contribution to the EPC, to characterize the nature of the EPC mechanism in *n*-doped diamond, supercell frozen phonon calculations for the LO phonon mode at the *X* point were performed. To incorporate the LO phonon at *X*, it is necessary to double the unit cell and

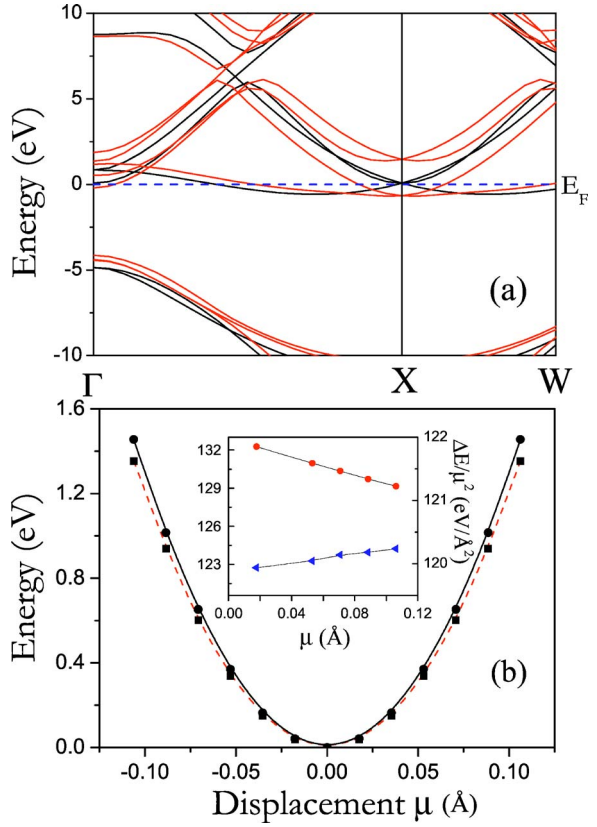

FIG. 9. (Color online) (a) Calculated band structure for n-doped diamond with e_v=4.03. In the presence of a frozen longitudinal optical phonon mode at X point of BZ with amplitude μ=0.07 Å the bands split (red solid lines). (b) Plots of the energy of distortion for the frozen longitudinal optical phonon mode at X point, for undoped diamond (solid circles) and n-doped diamond (solid square) with e_v=4.03. The black solid and red dashed lines are guides for the eye. Inset figure shows the plot of $\Delta E(\mu)/\mu^2$ with displacement μ, for pure diamond (red solid circles with right label) and n-doped diamond (blue left triangles with left label) with e_v =4.03.

reduce the crystal symmetry from *Fd*3*m* to *Pmma*. The electronic band structures of the undistorted and distorted (by displacing the appropriate atoms along the LO mode at X) are presented in Fig. 9(a). It is clear that the doubly degenerated electronic band at X point is perturbed significantly by the LO phonon vibration. This band splits into two bands, opening a large gap with the lower energy band crossing the Fermi surface. The crossing of the Fermi surface will result in large changes in the electronic structure, and therefore is possibly responsible for the strong EPC. To test the validity of this model, similar supercell calculations were also performed on the TA and TO phonons at the X point. In these cases, very small splittings in the bands are observed, thus indicating negligible contributions to the EPC process from both TO and TA vibrations. This conclusion is in complete agreement with the results of phonon linewidths [Fig. 7(b)].

The calculated change in energy versus atomic displacement (μ) of the LO mode at X point for pure and n-doped diamond is shown Fig. 9(b). In both cases, the energy versus μ is well described by the harmonic approximation $\Delta E(\mu) \propto \mu^2$. Lee *et al.*[6] reported a striking difference in the plot of $\Delta E(\mu)/\mu^2$ versus μ between pure and p-doped diamond. To investigate this effect in n-type diamond, $\Delta E(\mu)/\mu^2$ was plotted against μ as shown in the inset figure of Fig. 9(b). The difference between pure and n-doped diamond is indeed remarkable. While a negative (decreasing) linear behavior was found for pure diamond, apparently in agreement with the trend in p-doped diamond,[6] a positive and less linear behavior was observed for n-doped diamond. Therefore the mechanism described in p-doped diamond where the dominating EPC arises from optical phonon modes localized at the zone center may not be applicable for this new observation. The difference in the superconducting mechanism might originate from the significant difference in the electronic behaviors in these two doped systems as indicated in the band-structure calculation of Fig. 1.

To mimic the doped systems, both delocalized (VCA) and localized (supercell model) defect gave qualitatively similar results and both were successful in explaining the essential features of the superconductivity in B-doped diamond.[31] For example, as demonstrated here both the VCA and the supercell model within the rigid band approximation[8] predicted the increase in the EPC strength with the amount of doped holes. The experimentally observed decrease in superconducting temperature with pressure in B-doped diamond is in full accordance with the current VCA calculation. It was suggested[7,8] that the supercell method may be a more realistic model than a virtual crystal treatment. However, the supercell calculation of Lee *et al.*[6] on $C_{31}B$ has revealed strongly ordered (but unphysical) boron states. In contrast, coherent potential approximation alloy calculations[6] gave a largely similar electronic band structure as the virtual crystal model only with small disorder broadening. Experimentally the sharp Raman peak in pristine diamond was found to shift to lower frequency and becomes very broad[1] with increasing dc in B-doped diamond. The observed spectral feature is not supported by the supercell calculations.[8] In the supercell calculations,[8] apart from a strong softening of an optic mode, many residual C—C stretch bands still persist within the same frequency region as pure diamond. Even accounting for the breakdown of symmetry rules, these bands should remain strong in the Raman spectrum. Incidentally, the present VCA calculated spectral linewidth [Fig. 6(a)] of $\sim$80 cm^{-1} for the Raman mode agrees well with the observed width of the broad Raman band.[1]

IV. CONCLUSIONS

The electronic structure, lattice dynamics, and EPC of p-doped and n-doped diamonds have been studied using density functional theory within the VCA. For the current VCA calculation of p-doped diamond, the theory correctly reproduced all the essential properties of B-doped diamond such as the increase of lattice constant and the redshift of the Raman spectrum with increasing dopant concentration, and the pressure-induced decrease of T_c. The analysis of the spectral function for p-type diamond has shown that optical phonon modes dominate the EPC. It is predicted that λ and therefore the corresponding T_c should increase significantly

with increasing dc. The obvious agreement between theory and experiments for p-doped diamond supports the use of the VCA and the validity of the weak EPC BCS mechanism in p-type diamond.

From the VCA results of n-doped diamond, it is found that the superconducting temperature T_c is even higher than that in p-doped diamond at $dc > 2\%$. Thus it is indicated that n-type diamond might possess superconducting behavior as p-doped diamond does. The increase of λ with dc in n-doped diamond is attributed to phonon softenings and the increased electron density of states at the Fermi level. From phonon linewidth calculations, the LO phonon mode is found to dominate the EPC in n-doped diamond. This observation is substantiated by supercell frozen phonon band-structure calculations of the LO vibration at the X point. The mechanism of superconductivity in n-doped diamond is different from p-type diamond where the dominating EPC arises from optical phonon modes localized at the zone center. To verify the currently predicted superconductivity in n-doped diamond, the accurate experimental measurement on the n-doped diamonds with very high doping level ($\sim 10^{21}$ cm^{-3}) is needed. Although currently it is a great challenge to synthesize this high doping n-type diamond in experiments, experimentalists will continue pursuing the suitable impurities which help to realize the high level n-doping. As an alternative, we noticed that the observation of the superconductivity in the n-doped Si sp^3 network compound Ba_8Si_{46} has recently been reported.[32]

ACKNOWLEDGMENTS

This work was supported by the National Natural Science Foundation of China under Grant No. 10444001, the National Basic Research Priorities Program of China under Grant No. 2001CB711201, and the 973 Program under Grant No. 2005CB724400. Calculations in this work have been done using the PWSCF package.[33]

[1] E. A. Ekimov, V. A. Sidorov, E. D. Bauer, N. N. Mel'nik, N. J. Curro, J. D. Thompson, and S. M. Stishov, Nature (London) **428**, 542 (2004).

[2] Y. Takano, M. Nagao, I. Sakaguchi, M. Tachiki, T. Hatano, K. Kobayashi, H. Umezawa, and H. Kawarada, Appl. Phys. Lett. **85**, 2851 (2004).

[3] V. A. Sidorov, E. A. Ekimov, S. M. Stishov, E. D. Bauer, and J. D. Thompson, Phys. Rev. B **71**, 060502(R) (2005).

[4] E. Bustarret, J. Kačmarčik, C. Marcenat, E. Gheeraert, C. Cytermann, J. Marcus, and T. Klein, Phys. Rev. Lett. **93**, 237005 (2004).

[5] L. Boeri, J. Kortus, and O. K. Andersen, Phys. Rev. Lett. **93**, 237002 (2004).

[6] K. W. Lee and W. E. Pickett, Phys. Rev. Lett. **93**, 237003 (2004).

[7] H. J. Xiang, Z. Li, J. Yang, J. G. Hou, and Q. Zhu, Phys. Rev. B **70**, 212504 (2004).

[8] X. Blase, Ch. Adessi, and D. Connétable, Phys. Rev. Lett. **93**, 237004 (2004).

[9] G. Baskaran, cond-mat/0404286 (unpublished); cond-mat/0410296 (unpublished).

[10] K. Bharuth-Ram, A. Burchard, M. Deicher, H. Quintel, M. Restle, H. Hofsäss, and C. Ronning, Phys. Rev. B **64**, 195207 (2001); S. Prawer, C. Uzan-Saguy, G. Braunstein, and R. Kallish, Appl. Phys. Lett. **63**, 2502 (1993).

[11] M. Nesládek, K. Meykens, K. Haenen, L. M. Stals, T. Teraji, and S. Koizumi, Phys. Rev. B **59**, 14852 (1999); H. Sternschulte, K. Thonke, R. Sauer, and S. Koizumi, *ibid.* **59**, 12924 (1999); K. Okumura, J. Mort, and M. Machonkin, Appl. Phys. Lett. **57**, 1907 (1990).

[12] S. Koizumi, M. Kamo, Y. Sato, S. Mita, A. Sawabe, A. Reznik, C. Uzan-Saguy, and R. Kalish, Diamond Relat. Mater. **7**, 540 (1998).

[13] V. A. Nadolinny, A. P. Yelisseyev, J. M. Baker, D. J. Twitchen, M. E. Newton, A. Hofstaetter, and B. Feigelson, Phys. Rev. B **60**, 5392 (1999); R. Kalish, C. Uzan-Saguy, B. Philosoph, V. Richter, J. P. Lagrange, E. Gheeraert, A. Deneuville, and A. T. Collins, Diamond Relat. Mater. **6**, 516 (1997); E. Rohrer, C. F. O. Graeff, R. Janssen, C. E. Nebel, M. Stutzmann, H. Güttler, and R. Zachai, Phys. Rev. B **54**, 7874 (1996); S. Zhang, S. C. Ke, M. E. Zvanut, H. T. Tohver, and Y. K. Vohra, *ibid.* **49**, 15392 (1994).

[14] R. Job, M. Werner, A. Denisenko, A. Zaitsev, and W. R. Fahrner, Diamond Relat. Mater. **5**, 757 (1996).

[15] S. J. Sque, R. Jones, J. P. Goss, and P. R. Briddon, Phys. Rev. Lett. **92**, 017402 (2004); D. Segev and S.-H. Wei, *ibid.* **91**, 126406 (2003); L. G. Wang and A. Zunger, Phys. Rev. B **66**, 161202(R) (2002); Y. Miyamoto and M. Saito, *ibid.* **57**, 6527 (1998); Th. Frauenheim, G. Jungnickel, P. Sitch, M. Kaukonen, F. Weich, J. Widany, and D. Porezag, Diamond Relat. Mater. **7**, 348 (1998); G. Jungnickel, P. K. Sitch, Th. Frauenheim, B. R. Eggen, M. I. Heggie, C. D. Latham, and C. S. G. Cousins, Phys. Rev. B **57**, R661 (1998); S. J. Breuer and P. R. Briddon, *ibid.* **53**, 7819 (1995); R. Jonnes, J. E. Lowther, and J. Goss, Appl. Phys. Lett. **69**, 2489 (1996); A. B. Anderson, E. J. Grantscharova, and J. C. Angus, Phys. Rev. B **54**, 14341 (1996); C. Cunha, S. Canuto, and A. Fazzio, *ibid.* **48**, 17806 (1993); S. A. Kajihara, A. Antonelli, J. Bernholc, and R. Car, Phys. Rev. Lett. **66**, 2010 (1991).

[16] T. Tshepe, C. Kasl, J. F. Prins, and M. J. R. Hoch, Phys. Rev. B **70**, 245107 (2004).

[17] S. Baroni, P. Giannozzi, and A. Testa, Phys. Rev. Lett. **58**, 1861 (1987); P. Giannozzi, S. de Gironcoli, P. Pavone, and S. Baroni, Phys. Rev. B **43**, 7231 (1991).

[18] J. P. Perdew and K. Burke, Int. J. Quantum Chem. **57**, 309 (1996); J. P. Perdew, K. Burke, and M. Ernzerhof, Phys. Rev. Lett. **77**, 3865 (1996).

[19] N. Troullier and J. L. Martins, Phys. Rev. B **43**, 1993 (1991).

[20] F. D. Murnaghan, Proc. Natl. Acad. Sci. U.S.A. **30**, 244 (1944).

[21] Y. Ma, J. S. Tse, D. D. Klug, and R. Ahuja, Phys. Rev. B **70**, 214107 (2004); J. S. Tse, Z. Li, K. Uehara, Y. Ma, and R. Ahuja, Phys. Rev. B **69**, 132101 (2004).

[22] H. J. McSkimin and W. L. Bond, Phys. Rev. **105**, 116 (1957).

[23] O. A. Voronov and A. V. Rakhmanina, Inorg. Mater. **29**, 707 (1993).

[24] F. Brunet, A. Deneuville, P. Germi, M. Pernet, and E. Gheeraert, J. Appl. Phys. **81**, 1120 (1997).

[25] D. M. Teter and R. J. Hemley, Science **271**, 53 (1996).

[26] J. L. Warren, J. L. Yarnell G. Dolling, and R. A. Cowley, Phys. Rev. **158**, 805 (1967).

[27] Since the numerical calculations for the evaluation of the electronic structure and phonon calculation are different for metallic and insulating materials, we performed a series of phonon calculations at the zone center for metallic doped diamond with e_v in the range from 3.96 to 3.99, and then extrapolated the frequencies to the limiting value of $e_v=4$.

[28] W. L. McMillan, Phys. Rev. **167**, 331 (1968).

[29] P. B. Allen, Phys. Rev. B **6**, 2577 (1972); P. B. Allen and R. Silberglitt, *ibid.* **9**, 4733 (1974).

[30] T. Yildirim, O. Gülseren, J. W. Lynn, C. M. Brown, T. J. Udovic, Q. Huang, N. Rogado, K. A. Regan, M. A. Hayward, J. S. Slusky, T. He, M. K. Haas, P. Khalifah, K. Inumaru, and R. J. Cava, Phys. Rev. Lett. **87**, 037001 (2001).

[31] Please refer to this work and Refs. 5 and 6 for the VCA calculation; please refer to Refs. 7 and 8 for the supercell calculation.

[32] H. Kawaji, H. O. Horie, S. Yamanaka, and M. Ishikawa, Phys. Rev. Lett. **74**, 1427 (1995).

[33] S. Baroni, A. Dal Corso, S. de Gironcoli, and P. Giannozzi, http://www.pwscf.org